Seven-Band Complete Graphene Absorber Assisted by Metamaterial Concept for Optoelectronics and Engineering Technologies

Yousef Rafighirani[1], Javad Javidan[1], Hamid Heidarzadeh[1], Mousa Abdollahvand[1], Mohammad Alibakhshikenari[2], Patrizia Liveri[3]

[1] Department of Electrical and Computer Engineering, University of Mohaghegh Ardabili, Ardabil, Iran; rafighiraniyousef@gmail.com; javidan@uma.ac.ir; heidarzadeh@uma.ac.ir; m.abdollahvand@uma.ac.ir

[2] Department of Signal Theory and Communications, Universidad Carlos III de Madrid, 28911 Leganes, Madrid, Spain; mohammad.alibakhshikenari@uc3m.es

[3] Department of Engineering, University of Palermo, Palermo, IT 90128, Sicily, Italy; patrizia.livreri@unipa.it

***Abstract*- This paper reports a numerical study of a seven-band metamaterial absorber consisting of the round combination of the fundamental method to generate the maximum number of bands. The proposed structure consists of three layers, the absorber consists of a cut graphene layer, a gold layer on a silicon oxide dielectric layer with a cube-shaped cavity in the center. the structure has seven perfect absorption peaks, which are 91.2%, 99.5%, 97.7%, 94.3%, 97.8%, 91.1%, and 97.7% at 6.08 THz, 6.4 THz, 7.1THz, 7.32THz, 7.92THz, 9.21THz, and 9.66 THz, respectively. The seven-band absorbers obtained here have potential applications in many optoelectronics and engineering technology fields. One of the advantages of this structure compared to similar structures is its simplicity in design, which makes it possible to make this structure easily, combine the two methods used to create more bands. Absorption in multiple frequencies and the second method is to create cavities at different depths with different geometrical shapes in the dielectric, which can also achieve a high number of absorption peaks. It can be achieved by the use of layers with a small number, which provides a large number of absorption peak bands under these conditions, which have a higher number of peaks than many structures. The absorption values of this structure of all seven bands are above 90%, which enables maximum absorption in all frequencies .The proposed structure has the largest number of absorption bands, and also because of the high absorption that it has assigned, this structure can be a very suitable option for designing a seven-band absorber.**

***Keywords*- Metamaterial absorber, cut graphene layer, cube-shaped cavity.**

I. INTRODUCTION

In recent years, graphene-based metamaterial adsorbents have attracted the attention of many researchers. These absorbers are very attractive due to their high potential applications in optical electronics[1]. Some promising fields include photovoltaics and solar cells[2], biophotonic sensors[3], communication filters[3],[4], and selective frequency absorbers in the terahertz range. In the meantime, more attention is paid to sensors based on frequency absorbers[6]. With the advancement of technology, many improvements have been made in this field. Absorbers can minimize reflection and transmission to achieve complete absorption, the waves absorb more than 90% of the incident waves and complete absorption occurs typically, a classical absorber consists of three layers. These three layers are usually made of a perfect conductor, dielectric, and metamaterial[7].

Metamaterials are artificially engineered materials that do not exist naturally. They are made from existing materials and exhibit extraordinary electromagnetic properties such as inverse Doppler effects, negative refractive indices, or electromagnetic shielding[8], [9]. Graphene is one of the popular metamaterials. It is a layer of graphite with a thickness of one atom, in which the atoms are arranged in a hexagonal pattern. There are strong covalent bonds between each carbon atom [10]. The applications of graphene are seen in various industries from medicine to engineering because of its unique properties such as thermal, physical, chemical, optical, and electromagnetic properties [11], [12].

In the last decade, many studies have been carried out on graphene-based terahertz absorbers. Therefore, a lot of progress has been made in this field. The sensors can work on different microwave frequencies[13], [14].

Terahertz absorbers based on graphene can be classified into two groups: Broadband[15] and narrowband[16].

The terahertz absorbers based on graphene are mostly designed in two bands[17], three bands[18],[19], and four absorption bands[20], [21] Current structures are mostly no more than four. More importantly, in this structure, seven bands have been designed with complete absorption, resulting from combining two fundamental methods to design frequency absorbers.

Narrowband absorbers are very suitable for applications such as biosensors because they have a narrow bandwidth and high sensitivity. Narrowband sensors operate based on refractive index (RI) and have found applications in the field such as biochemical and biomedical sensing. terahertz biosensors are becoming increasingly popular due to their portability, small size, reproducibility, ease of use, high detection capability, and cost-effectiveness are becoming increasingly popular. Moreover, terahertz sensor fabrication technology is progressing rapidly [22]. Therefore, graphene-based terahertz-perfect absorbers are good proposals for RI sensing.

Maxwell's equations play a fundamental role in describing light propagation and electromagnetic properties. These equations, formulated by James Clark Maxwell, allow us to predict the behavior of light in different environments. In the case of lossless dielectric media, Maxwell's equations can be expressed in a simpler form because these media have no energy losses. On the other hand, the Schrödinger equation, which is used to study electronic states in solids, can also be used to study photon states in photonic crystals. The major difference is that electrons are described by a complex scalar field and interact with each other, while a real vector field defines photons and do not interact with each other. As a result, solving the equations related to photons can lead to a precise description of their properties, so that the results of computer simulations can be as accurate as laboratory experiments[23].

Multi-layer frequency absorbers are used in various applications, including microwave, radar, and telecommunications. The absorption mechanism of multi-layer frequency absorbers is such that the underlying conductive layer does not allow radiation to pass through the structure. In addition, the middle dielectric layer and the metamaterial placed on the dielectric should also be designed so that the waves reflected from inside the structure have a phase difference. This phase difference neutralizes each other and in order to achieve complete absorption, an optimal structure is created. These absorbers are composed of different layers; each layer has a specific role in absorbing waves. In general, the structure of a multilayer absorber includes the following:

Conductive Layer: This layer is located in the lowest part of the absorber and is made of conductive materials such as metals. The main task of this layer is to absorb electromagnetic energy and convert it into heat.

Dielectric layer: This layer is above the conductive layer and is made of dielectric materials such as resins, plastics or carbon fiber. The main task of this layer is to absorb electromagnetic waves and convert them into heat.

Metamaterial Layer: This layer is located in the highest part of the absorber and consists of metamaterial structures. Metamaterials have unusual properties that are specifically designed to absorb electromagnetic waves. This layer can selectively absorb the waves and convert them into heat[24].

II. Design And Analysis Of Biosensor

By combining these layers, multilayer absorbers can completely absorb electromagnetic waves and reduce unwanted interference. These structures are widely used in telecommunication equipment, radars, and microwave devices.

In the proposed structure, a combination of two methods has been used to create an absorption band, so that by combining these two methods, the number of absorption bands and also a high absorption value have been achieved.

Surface plasmons, which form at the interface between a metal and a dielectric, react strongly with polarized light and are involved in surface plasmon resonance (SPR). For a better understanding of surface plasmons, the behavior of metals against light electromagnetic fields and their dielectric performance should be investigated, because these factors are influential in the optical properties of metals.

This boundary is usually between a metal and a dielectric with a small imaginary dielectric constant (positive real part) and a large real dielectric constant (negative imaginary part). Surface plasmons react to light in the visible range of the electromagnetic spectrum and are used in applications such as surface plasmon resonance (SPR). The dielectric performance of plasmon plays an important role in the optical properties of metals. The movement of charge in a surface plasmon always creates electromagnetic fields outside (as well as inside) the metal. This phenomenon is also studied as surface plasmon resonance (SPR). Surface plasmons play an important role in various technologies, including information transmission in nanostructures, similar to photonics.

In the field of nanotechnology, the phenomenon of localized surface plasmon resonance (LSPR) plays an important role in the manipulation of light at the nanoscale. When nanomaterials interact with electromagnetic waves at their resonant frequency, LSPR occurs, leading to enhanced light-matter interactions. By modifying the dielectric properties around the nanoparticles, we can tune the LSPR frequency and control the absorption and scattering of light. This capability has various applications in measuring, imaging and optical devices with nanoscale features. Researchers are investigating new nanostructures to further enhance LSPR effects and exploit them for advanced technological purposes[25].

Due to their small dimensions, nanoparticles have different properties compared to larger-volume atoms. The surface characteristics of nanoparticles, including their electromagnetic characteristics and resonances, are very important in their behavior and reaction to the environment and external forces. For example, the size and shape of nanoparticles can affect the electromagnetic radiation that interacts with them.

Also, the existence of a special map between the surface of nanoparticles and their properties with the dielectric of the environment and metal indicates the importance and many effects that may play a role in the behavior of nanoparticles.

Finally, slight changes in the dielectric properties around a nanoparticle can affect its resonance and surface properties and cause a change in the optical and electromagnetic behavior of nanoparticles. These phenomena are investigated in research related to surface plasmons and their various applications.

The proposed structure consists of three layers. As shown in Figure 1 (b), the absorber consists of a cut graphene layer and a gold layer placed on the silicon oxide dielectric layer. The top layer is a 1 nm thick graphene layer with relaxation time $\tau = 1.8ps$, temperature of 300 K, and chemical potential $\mu_c = 0.5eV$. In the production process, silicon is placed on one side of the gold layer with the purpose of chemical vapor deposition, and according to Figure 1 (a), a cube-shaped hole with sides of 0.75 µm and a depth of 3 µm is created inside it, on the other side, a graphene sheet is placed on silicon dioxide with a thickness of 0.2 µm. The raised side meter is placed on the hollow side. There is a vacuum inside the cavity.

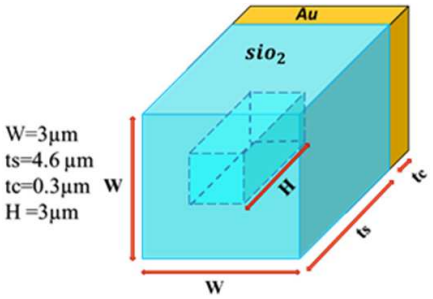

(a)

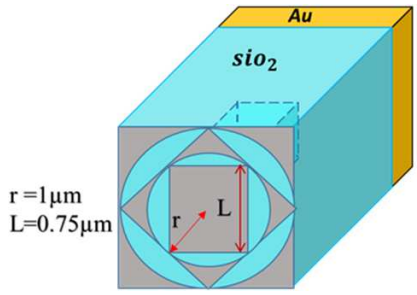

(b)

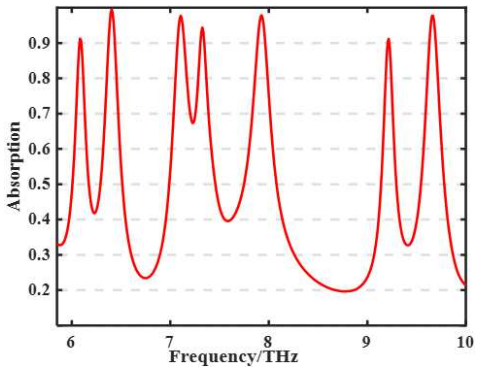

(c)

Fig.1. Figure 1. (a) Structure of a conductor along with a dielectric with a hole created in the center. (b) Proposed overall structure. (c) absorption wave output of the proposed structure at seven different frequencies.

The dielectric layer can be deposited in a sintering process in a vacuum chamber. Then, a standard photolithography process can be used to obtain the top pattern of graphene and implement the cut structure of graphene [26], [27]. Through a lot of trial and error, we arrived at the best parameters as follows: the thickness of the silicon dioxide is ts=4.6 μm and the thickness of the gold layer used in the bottom layer is tc=0.3 μm. In this article, the difference in the absorption coefficient value is solved using the time domain method, which is calculated by the formula $A = 1 - S_{21}^2 - S_{11}^2$. Because the bottom layer of our structure is composed of gold, it prevents the return of electromagnetic waves, so the incoming wave is absorbed as much as possible, more precisely, the transmission can be ignored, to be more precise $A = 1 - S_{11}^2$ [28]. In addition, this paper has chosen PML conditions in the z-direction and periodic boundary conditions in the x and y-directions.

III. Results and Discussions

To get the final structure, start from a simple structure, check different conditions in terms of dimensions and parameters, and design the final structure. To reach the final structure, the goal is to achieve maximum absorption. Design and analysis have been done with computer simulation software (CST) and all dimensional parameters are selected by trial and error. In all designs, the conductivity value of the conductor (gold) $\sigma = 4.7 \times 10^7 S/m$ [29]and for the dielectric layer of silicon dioxide, $\varepsilon = 3.9$ transmission coefficient [30].

As in Figure 1(c), the output of the absorption spectrum the structure has seven perfect absorption peaks, which are 91.2%, 99.5%, 97.7%, 94.3%, 97.8%, 91.1%, and 97.7% at 6.08 THz, 6.4 THz, 7.1THz, 7.32THz, 7.92THz, 9.21THz, and 9.66 THz, respectively.

In order to reach the desired ideal structure, different values have been given for all the variables of the structure, several variables are mentioned in Figure 2.

As in Figure 2 (a), the output of the absorption spectrum is in seven frequency bands for different amounts of graphene relaxation time, respectively, τ=1.6μm, τ=1.7μm, τ=1.8μm, τ=1. 9μm. It has been quantified and it can be seen that at the value of m, τ=1.8μm, the absorption spectrum has seven absorption peaks with the highest absorption value and the amount of relaxation time is determined with the help of the absorption spectrum.

As can be seen in Figure 2 (b), the output absorption spectrum is in seven frequency bands for different values of the chemical potential of graphene, which are μ =0.3eV, μ =0.4eV, μ =0.5eV, μ =0.55eV, respectively. It has been quantified and in the value of μ =0.5eV, the absorption spectrum has seven absorption peaks with the highest absorption value, and the most ideal value is determined.

Figure 2(c) shows the frequency absorption spectrum with the change in the values of H, which is in the depth structure of the cubic cavity created in the center of the dielectric, for different values of H=3.5 μm, H=3μm, H=2.5 μm. It has been shown that the depth of the hole in the value of H=3μm, shows the most suitable absorption output.

Meanwhile, the surface of the hole is covered with silicon dioxide with a thickness of 0.2 µm so that cut graphene can be grown on it.

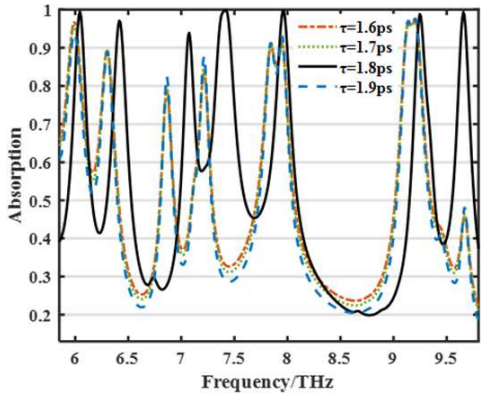

(a)

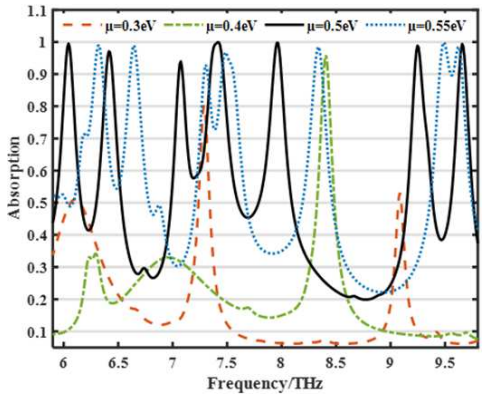

(b)

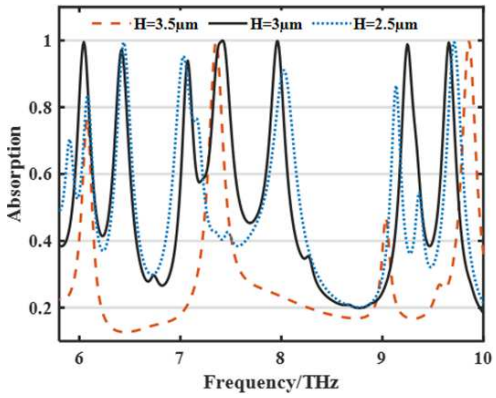

(c)

Fig.2. Figure 2. Output absorption spectrum for (a) different values of relaxation time for graphene (b) with different values of chemical potential of graphene (c) different values of hole depth in dielectric.

Figure 3 shows the electric field distributions [real (Ez)] in the natural incidence of TE. Waves at absorption peak frequencies. As you can see in Figure 3(a), the field distribution is mainly concentrated in the two corners located along the graphene junctions in the x direction, which is the first resonance at the frequency of 6.08 THz. It is due to resonance in these points. Figure 3b shows that the electric field is mainly spread in other parts and to other junctions, for which a frequency of 6.4 THz is attributed. In Figure 3 (c), the field tends to the y direction and is more intense in the connecting parts of graphene, which is attributed to a frequency of 7.1 THz.

In Figure 3 (d), the field is completely inclined to the y direction and it is more intense in the connection parts in the y direction of the graphene, which has a frequency of 7.32 THz.

TABLE I: Comparison between the features of the absorber structure of different articles with the features of the proposed absorber structure in this paper

FEATURE REFERENCE	ABSORPTION FREQ. (THZ)	ABSORPTION PEAK(%)
[31]	0.60 THz 0.80 THz 1.74 THz 2.33 THz 2.75 THz 3.63 THz	99.10% 99.90% 98.77% 98.82% 99.99% 99.63%
[32]	1.054 THz 2.16 THz 3.59 THz 3.87 THz	90.6% 97.2% 93.95% 99.61%
[33]	0.80 THz 2.89 THz 3.98 THz 4.36 THz	IN AN AVERAGE OF 97.54%
[34]	1.92 THz 4.62 THz 8.81 THz	98.4% 98.3% 99.6%
[35]	4.24 THz 5.89 THz 9.66 THz 10.62 THz	99.5% 99.7% 94.71% 97.06%
PROPOSED ABSORBER	6.08 THz 6.4 THz 7.1THz 7.32THz 7.92THz 9.21THz 9.66 THz	91.2% 99.5% 97.7% 94.3% 97.8% 91.1% 97.7%

Figure 3 (e) the electric field is deviated from the y direction and is more concentrated at the edges of the graphene slices, which shows a frequency of 7.92 THz.

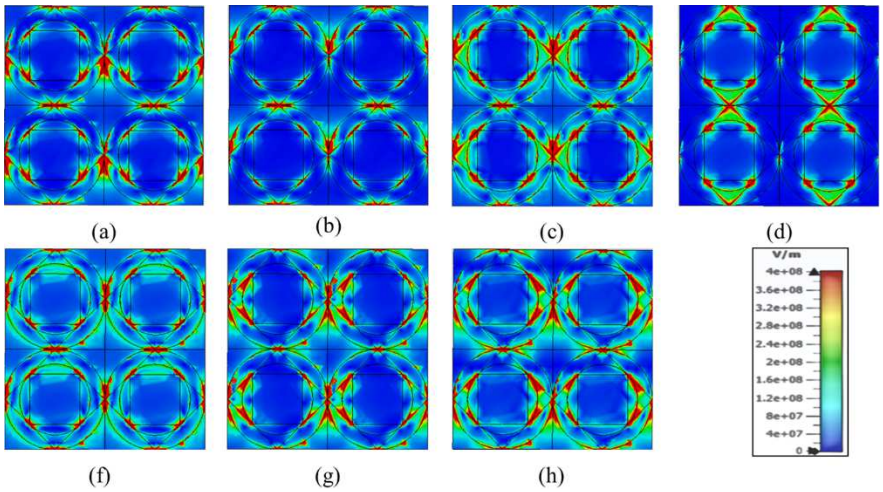

Fig.3. Figure 3.Electric feld [real (Ez)] distributions in the normal incidence of TE waves at frequencies of (a) 6.08 THz, (b) 6.4 THz, (c) 7.1 THz, (d) 7.32 THz, (e) 7.92 THz, (f) 9.21 THz, and (h) 9.66 THz.

In Figure 3(f) is more inclined to the X axis, the field density is at the cut edges of graphene and the frequency is 9.21 THz for this state. In Figure 3(h), the field concentration is higher in the x direction, and the frequency of 9.66 THz is attributed to it. One of the advantages of this structure compared to similar structures is its simplicity in design, which makes it possible to make this structure easily, combine the two methods used to create more bands. Absorption in multiple frequencies and the second method is to create cavities at different depths with different geometrical shapes in the dielectric, which can also achieve a high number of absorption peaks. It can be achieved by the use of layers with a small number, which provides a large number of absorption peak bands under these conditions, which has a higher number of peaks than many structures, which is very suitable for filtering telecommunication signals and thermal imaging. The absorption values of all seven bands of this structure are above 90%, which enables maximum absorption in all frequencies. As it is clear from Table 1, the proposed structure has the largest number of absorption bands and also because of the high absorption that it has allocated, this structure can be a very suitable option for designing a seven-band absorber.

IV. Conclusion

In recent years, many terahertz absorbers have been introduced. Adsorbent was provided .In this paper, there is a complete seven-band metamaterial absorber, which has a proposed structure consisting of three layers, the absorber is made of a cut graphene layer, a gold layer placed on a silicon oxide dielectric layer, with a cube-shaped cavity in the center. Given is formed. the structure has seven perfect absorption peaks, which are 91.2%, 99.5%, 97.7%, 94.3%, 97.8%, 91.1%, and 97.7% at 6.08 THz, 6.4 THz, 7.1THz, 7.32THz, 7.92THz, 9.21THz, and 9.66 THz, respectively. The proposed structure has the largest number of absorption bands, and also because of the high absorption that it has allocated, this structure can be a very suitable option for designing a seven-band absorber. The seven-band absorbers obtained here have potential applications in many optoelectronics and engineering technology fields. One of the advantages of this structure compared to similar structures is simplicity in design, which makes it possible to build this structure easily.

ACKNOWLEDGMENT

Dr. Mohammad Alibakhshikenari acknowledges support from the CONEX-Plus programme funded by Universidad Carlos III de Madrid and the European Union's Horizon 2020 research and innovation programme under the Marie Sklodowska-Curie grant agreement No. 801538.

REFERENCES

[1] M. Y. Azab, M. F. O. Hameed, A. M. Nasr, and S. S. A. Obayya, "Highly sensitive metamaterial biosensor for cancer early detection," *IEEE Sensors Journal*, vol. 21, no. 6, pp. 7748–7755, 2021.

[2] M. Götz, N. Osterthun, K. Gehrke, M. Vehse, and C. Agert, "Ultrathin nano-absorbers in photovoltaics: Prospects and innovative applications," *Coatings*, vol. 10, no. 3, p. 218, 2020.

[3] L. Marcu, S. A. Boppart, M. R. Hutchinson, J. Popp, and B. C. Wilson, "Biophotonics: the big picture," *Journal of biomedical optics*, vol. 23, no. 2, pp. 021103–021103, 2018.

[4] S. G. Shafagh, H. Kaatuzian, and M. Danaie, "Design and Analysis of Infrared Tunable All-Optical Filters Based on Plasmonic Hybrid Nanostructure Using Periodic Nanohole Arrays," *Plasmonics*, vol. 17, no. 2, pp. 693–708, Apr. 2022, doi: 10.1007/s11468-021-01558-8.

[5] Z. Zhang, F. Shi, and Y. Chen, "Tunable Multichannel Plasmonic Filter Based on Coupling-Induced Mode Splitting," *Plasmonics*, vol. 10, no. 1, pp. 139–144, Feb. 2015, doi: 10.1007/s11468-014-9787-z.

[6] Y. Rafighirani, J. Javidan, and H. Heidarzadeh, "Polarization-independent tunable multi-band terahertz absorber based on graphene structure to design the ultra-high sensitive biosensors," *Physica Scripta*, vol. 99, no. 7, p. 075014, 2024.

[7] G. M. Akselrod *et al.*, "Large-area metasurface perfect absorbers from visible to near-infrared," *Advanced Materials*, vol. 27, no. 48, pp. 8028–8034, 2015.

[8] P. Zamzam, P. Rezaei, O. Mohsen Daraei, and S. A. Khatami, "Band reduplication of perfect metamaterial terahertz absorber with an added layer: cross symmetry concept," *Opt Quant Electron*, vol. 55, no. 5, p. 391, May 2023, doi: 10.1007/s11082-023-04561-x.

[9] M. Bennaoum, M. Berka, A. Bendaoudi, A. Y. Rouabhi, and Z. Mahdjoub, "Investigation of a Near-Perfect Quad-Band Polarization-Insensitive Metamaterial Absorber Based on Dual-T Circular Shaped Resonator Array Designed on a Silicon Substrate for C-, X- and Ku-bands Applications," *Silicon*, vol. 15, no. 2, pp. 699–712, Jan. 2023, doi: 10.1007/s12633-022-02038-2.

[10] N. Sharma, R. D. Gupta, R. C. Sharma, S. Dayal, and A. S. Yadav, "Graphene: An overview of its characteristics and applications," *Materials Today: Proceedings*, vol. 47, pp. 2752–2755, 2021.

[11] D. Shekhawat and R. Mehra, "Design of Ultra-Compact and Highly-Sensitive Graphene Assisted Silicon Micro-Ring Resonator Modulator for Switching Applications," *Silicon*, vol. 14, no. 8, pp. 4383–4390, Jun. 2022, doi: 10.1007/s12633-021-01219-9.

[12] P. Upender and A. Kumar, "Quad-Band Circularly Polarized Tunable Graphene Based Dielectric Resonator Antenna for Terahertz Applications," *Silicon*, vol. 14, no. 10, pp. 5513–5526, Jul. 2022, doi: 10.1007/s12633-021-01336-5.

[13] S. Khani, A. Farmani, and P. Rezaei, "Optical Resistance Switch for Optical Sensing," in *Optical Imaging and Sensing*, 1st ed., J. Wu and H. Xu, Eds., Wiley, 2023, pp. 83–122. doi: 10.1002/9783527835201.ch4.

[14] S. Kiani, P. Rezaei, and M. Fakhr, "Dual-frequency microwave resonant sensor to detect noninvasive glucose-level changes through the fingertip," *IEEE Transactions on Instrumentation and Measurement*, vol. 70, pp. 1–8, 2021.

[15] B. Khodadadi, P. Rezaei, V. Ghods, and M. Babaeinik, "Wideband polarization-insensitive metamaterial perfect absorber based on bilayer graphene metasurface," *Opt Quant Electron*, vol. 54, no. 11, p. 739, Nov. 2022, doi: 10.1007/s11082-022-04136-2.

[16] A. N. Razani and P. Rezaei, "Multiband Polarization Insensitive and Tunable Terahertz Metamaterial Perfect Absorber Based on The Heterogeneous Structure of Graphene," 2021, Accessed: Feb. 12, 2024. [Online]. Available: https://www.researchsquare.com/article/rs-438846/latest

[17] M. Nejat and N. Nozhat, "Ultrasensitive THz refractive index sensor based on a controllable perfect MTM absorber," *IEEE sensors journal*, vol. 19, no. 22, pp. 10490–10497, 2019.

[18] B. Khodadadi, M. Babaeinik, V. Ghods, and P. Rezaei, “Triple-band metamaterial perfect absorber for refractive index sensing in THz frequency,” *Opt Quant Electron*, vol. 55, no. 5, p. 431, May 2023, doi: 10.1007/s11082-023-04684-1.

[19] M. Biabanifard, A. Arsanjani, M. S. Abrishamian, and D. Abbott, “Tunable terahertz graphene-based absorber design method based on a circuit model approach,” *IEEE Access*, vol. 8, pp. 70343–70354, 2020.

[20] A. Hamouleh-Alipour, A. Mir, and A. Farmani, “Analytical modeling and design of a graphene metasurface sensor for thermo-optical detection of terahertz plasmons,” *IEEE Sensors Journal*, vol. 21, no. 4, pp. 4525–4532, 2020.

[21] S. K. Patel *et al.*, “Graphene based highly sensitive refractive index sensor using double split ring resonator metasurface,” *Opt Quant Electron*, vol. 54, no. 3, p. 203, Mar. 2022, doi: 10.1007/s11082-022-03600-3.

[22] A. N. Razani, P. Rezaei, P. Zamzam, S. A. Khatami, and O. M. Daraei, “Absorption-based ultra-sensitive RI sensor based on the flower-shaped graphene resonator for early detection of cancer,” *Optics Communications*, vol. 524, p. 128775, 2022.

[23] J. D. Joannopoulos, S. G. Johnson, J. N. Winn, and R. D. Meade, “Molding the flow of light,” *Princet. Univ. Press. Princeton, NJ [ua]*, 2008, Accessed: Feb. 27, 2024. [Online]. Available: https://physics.mit.edu/wp-content/uploads/2021/01/physicsatmit_01_joannopolous.pdf

[24] V. B. Shalini, “A polarization insensitive miniaturized pentaband metamaterial THz absorber for material sensing applications,” *Opt Quant Electron*, vol. 53, no. 5, p. 213, May 2021, doi: 10.1007/s11082-021-02898-9.

[25] M. Shahmansouri, R. Aboltaman, and A. P. Misra, “Surface plasmons in a semi-bounded massless Dirac plasma,” *Physics Letters A*, vol. 382, no. 32, pp. 2133–2136, 2018.

[26] N. T. Tung, “Lithographic fabrication and spectroscopic characterization of a THz metamaterial absorber,” *Vietnam Journal of Science and Technology*, vol. 59, no. 1, pp. 40–46, 2021.

[27] X. Shen *et al.*, “Triple-band terahertz metamaterial absorber: Design, experiment, and physical interpretation,” *Applied Physics Letters*, vol. 101, no. 15, 2012, Accessed: May 21, 2024. [Online]. Available: https://pubs.aip.org/aip/apl/article/101/15/154102/150835

[28] S.-Y. Chiam, R. Singh, C. Rockstuhl, F. Lederer, W. Zhang, and A. A. Bettiol, “Analogue of electromagnetically induced transparency in a terahertz metamaterial,” *Phys. Rev. B*, vol. 80, no. 15, p. 153103, Oct. 2009, doi: 10.1103/PhysRevB.80.153103.

[29] J. Tian, R. Ke, R. Yang, and W. Pei, “Tunable quad-band perfect metamaterial absorber on the basis of monolayer graphene pattern and its sensing application,” *Results in Physics*, vol. 26, p. 104447, 2021.

[30] P.-Y. Chen and A. Alù, “Atomically Thin Surface Cloak Using Graphene Monolayers,” *ACS Nano*, vol. 5, no. 7, pp. 5855–5863, Jul. 2011, doi: 10.1021/nn201622e.

[31] B.-X. Wang, G.-Z. Wang, T. Sang, and L.-L. Wang, “Six-band terahertz metamaterial absorber based on the combination of multiple-order responses of metallic patches in a dual-layer stacked resonance structure,” *Scientific reports*, vol. 7, no. 1, p. 41373, 2017.

[32] B. Appasani, P. Prince, R. K. Ranjan, N. Gupta, and V. K. Verma, “A Simple Multi-band Metamaterial Absorber with Combined Polarization Sensitive and Polarization Insensitive Characteristics for Terahertz Applications,” *Plasmonics*, vol. 14, no. 3, pp. 737–742, Jun. 2019, doi: 10.1007/s11468-018-0852-x.

[33] P. Lou, B.-X. Wang, Y. He, C. Tang, Q. Niu, and F. Pi, “Simplified Design of Quad-Band Terahertz Absorber Based on Periodic Closed-Ring Resonator,” *Plasmonics*, vol. 15, no. 6, pp. 1645–1651, Dec. 2020, doi: 10.1007/s11468-020-01184-w.

[34] M. Rahmanshahi, S. Noori Kourani, S. Golmohammadi, H. Baghban, and H. Vahed, “A Tunable Perfect THz Metamaterial Absorber with Three Absorption Peaks Based on Nonstructured Graphene,” *Plasmonics*, vol. 16, no. 5, pp. 1665–1676, Oct. 2021, doi: 10.1007/s11468-021-01432-7.

[35] A. Norouzi-Razani and P. Rezaei, “Multiband polarization insensitive and tunable terahertz metamaterial perfect absorber based on the heterogeneous structure of graphene,” *Opt Quant Electron*, vol. 54, no. 7, p. 407, Jul. 2022, doi: 10.1007/s11082-022-03813-6.